Clinical PET Imaging with the C-PET Camera

Sean L. Riggin, Kevin J. Kilroy and Robin J. Smith

Division of Nuclear Medicine, Department of Radiology, Hospital of the University of Pennsylvania, Philadelphia, Pennsylvania

Objective: Clinical PET studies require a high-performance and user-friendly PET camera. The C-PET camera uses a simple design and a large field of view for these purposes.

Methods: We describe the camera features, daily quality control, and routine clinical study preparation, performance, processing and presentation from the technologist's perspective.

Results: The C-PET camera is used for whole-body cancer, cardiac and brain imaging. It operates clinically near its peak performance. The 25.6-cm axial field of view (FOV), lack of interplane septa and singles transmission capability allow 70 cm of the body to be surveyed in less than 1 h with good image quality. Quality control procedures take 30 min per day. Clinical scans and image processing are menu driven, allowing the technologist to perform several tasks simultaneously. Fully corrected images typically are available for physician review within 1 h of acquisition. The current procedures are outlined.

Conclusion: The C-PET camera uses a clinically oriented design for rapid acquisition and presentation of high-quality PET images. Operation is straightforward and user-friendly.

Key Words: positron emission tomography; quality control; cancer imaging

PET rapidly is becoming a clinical modality for assessing cancer (*1,2*), trauma, cardiac viability and patients with intractable seizures. More medical centers and radiology practices are considering the purchase of a dedicated PET camera (*3–6*) or a coincidence detection system (*7–9*) as the demand increases for PET studies, particularly ^{18}F-fluorodeoxyglucose studies. Whole-body surveys of cancer patients have emerged as the most common PET study. This is because ^{18}F-FDG PET is currently the most sensitive, specific and noninvasive imaging test for detecting and staging cancer. It can distinguish tumors from normal tissue and monitor tumor response to therapy early in the course of treatment.

The Institute for Clinical PET estimates that 540,000 PET studies per year are indicated for cancer, making more than 260,000 other diagnostic procedures unnecessary. Even at a cost of $1700 per PET study, this would result in a savings of $3.3 billion per year, while improving patient comfort, management and outcome.

PET is a powerful and valuable technique in clinical oncology because it images the physiologic activity or malignancy of tumors directly with high sensitivity anywhere in the body. Whole-body PET surveys using FDG visualize the glucose or glycolytic activity of tumors by their uptake. This uptake normalized to injected dose per weight of patient (mCi/kg) provides an index called the standardized uptake value (SUV), which has been found to correlate well with tumor metabolic rates and, therefore, malignancy. Since the first clinical whole-body PET oncology studies were performed in 1990 this application has come to comprise 80% of PET studies at the 55 US and the nearly 100 PET centers outside the US.

PET also is used clinically to evaluate cardiac patients for bypass surgery or transplant by assessing the viability of the myocardium to be reperfused. PET studies of the brain include evaluating brain trauma, seizures and tumors, both before and after treatment.

In deciding on a camera system for clinical studies consideration should be given to both the capabilities and cost of operating the camera. While dual-headed coincidence systems are less expensive, they also are more limited in application. Top-of-the-line research-oriented PET cameras have excellent performance, however, they often are prohibitively expensive to purchase and operate. The C-PET (UGM ADAC, Philadelphia, PA) camera is a popular choice because it is a powerful and reliable clinical PET camera while being economical to purchase and operate.

MATERIALS AND METHODS

The performance characteristics of the C-PET camera are summarized in Table 1. The camera consists of 6 large curved planar detectors of NaI(Tl) with 288 photomultiplier tubes and uses positioning algorithms similar to those used in digital Anger cameras (*10*). The camera has a 25.6-cm axial and 57.6-cm transaxial field of view (FOV) and operates without interplane septa. This gives the camera a high geometric sensitivity and allows the torso to be surveyed with few bed positions (*6,11*). The camera also uses a 4-mCi point source of

For correspondence or reprints contact: Sean L. Riggin, Division of Nuclear Medicine, Department of Radiology, Hospital of the University of Pennsylvania, 3400 Spruce St., Philadelphia PA 19104; Phone: 215–662–7662; E-mail: sean@oasis.rad.upenn.edu.

TABLE 1
C-PET Performance Characteristics

Parameter	C-PET performance
Axial FOV	25.6 cm
Transaxial FOV	57.6 cm
Energy resolution	12%
Spatial resolution	5.1 mm FWHM
Sensitivity	400 kcps/μCi/cc
Scatter fraction	29%
FDG injection	0.068 mCi/kg
Peak counting rates (emission)	85 kcps (body), 120 kcps (brain)
Counting rates (transmission)	210 kcps (180–240 kcps)
Rebinning	Fourier rebin (3-D to 2D)
Reconstruction	OS-EM (4 iterations, 8 subsets)

[137]Cs for postinjection transmission measurements (12,13). This takes advantage of the intense flux of single photons to perform transmission scans in 1–2 min. The axial FOV for this point transmission source is 11.2 cm, about the center of the axial FOV, so that axial bed movements of 11.2 cm are used when performing body surveys. The advantages of this camera are that it operates clinically near its peak counting rate performance (with 1.0–1.5 mCi of activity in the FOV) and has a simple and reliable design. The camera is menu driven for both acquisition and reconstruction (using predefined protocols and a file manager system) and routinely provides attenuation-corrected images. The disadvantages are that randoms and scatter correction currently use a profile subtraction method (10) that requires the technologist to draw elliptical regions approximating the body outline on 5–10 transaxial slices of the nonattenuation-corrected images.

TABLE 2
Five Quality Control Tests

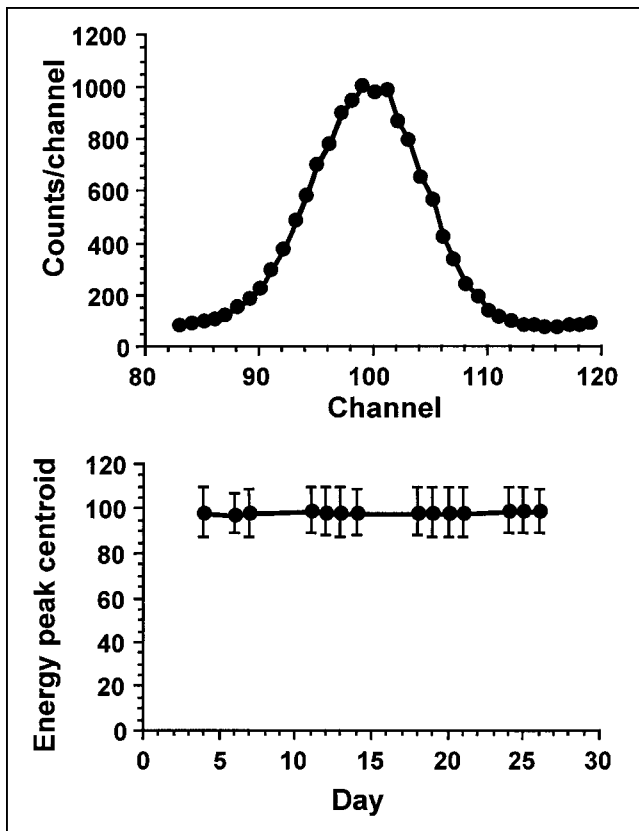| QC test	Parameter tested	Duration
PM tube baseline signals	Signal integrity, PMT function	30 s
Energy spectra	Energy signal, PMT gain matching	30 s
[68]Ge or [22]Na line source scans (0, $\pm$5, $\pm$10 cm in 25.6 cm FOV)	Spatial distortion correction	5 min
[137]Cs point singles blank scan	Detector uniformity and sensitivity	5 min
Uniformly filled cylinder (30 M cts emission scan)	Image nonuniformity	15 min

Once every 6–8 mo, the manufacturer or an on-site physicist performs the quality control procedures of generating: (a) normalization files used to correct for residual nonuniformities of detector response; (b) blank scans (or transmission scans with no object in the FOV) used to normalize transmission scans; and (c) calibration files used to convert image count density to activity concentration by correcting studies for camera deadtime. All acquisitions and reconstructions use predefined protocols. These allow the technologist to input patient details (name, weight, amount of radioactivity administered, radiopharmaceutical, comments, PET study identifier, etc.), position the patient and start the imaging study within minutes. The technologist's tasks in performing routine camera quality control and clinical study acquisition and processing are described below (14).

Five-Step Quality Control

Daily quality control consists of the 5 tests described in Table 2. The photomultiplier tube (PMT) baseline signals test (quality control Test #1 (Fig. 1)) checks that all the camera components are connected (control and data signals pass back and forth) and that the PMTs are functioning well. The baseline signals are the dark noise in the PMT signals in the absence of radioactivity in the FOV and, thus, of scintillation light in the detectors. A range of values (arbitrary units) between 15 and 40 are acceptable and
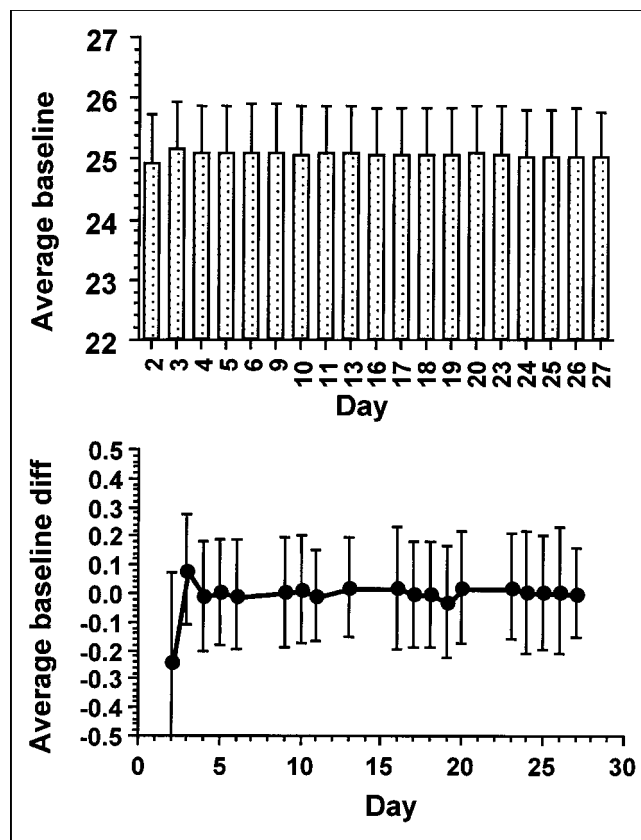
FIGURE 1. Summary of C-PET quality control. Top: Average baselines across 288 PMTs against days. Error bars are standard deviations across PMTs. Bottom: Average day-to-day differences in baselines for each PMT. Error bars are standard deviations of these differences. Note baseline differences are typically less than 0.5%.

FIGURE 2. Summary of C-PET quality control. Top: Example of an energy spectrum from a ^{68}Ge line source (511-keV photons) for a detector with a 12% FWHM resolution. Bottom: Energy peak centroids measured on successive days. Error bars are FWHM for the detector.

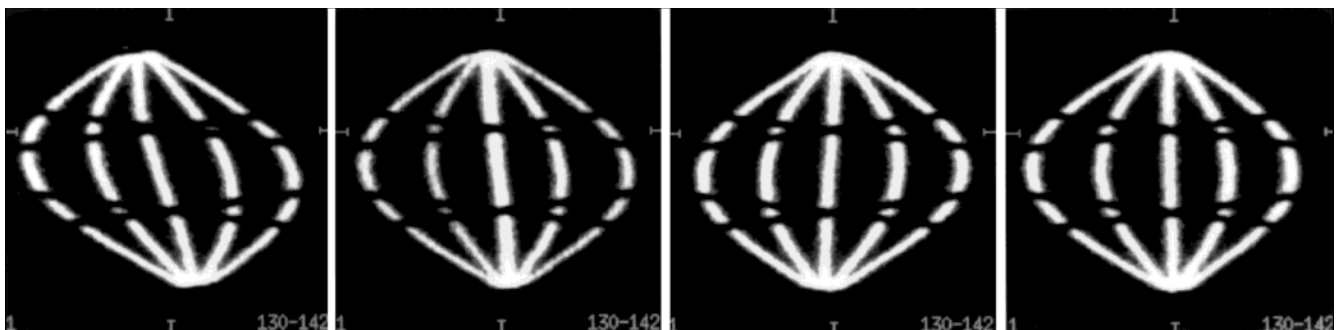centroid. Either change would result in more events falling outside the narrow energy windows of the C-PET camera.

The ^{68}Ge or ^{22}Na line source scans (quality control Test #3 (Fig. 3)) are acquired at 5 radial positions across the 25.6-cm diameter FOV and test that the position calculations with distortion correction are correct. The sine curves for the individual lines should be continuous and without any kinks indicative of uncorrected distortion.

The acquisition of a daily blank scan (quality control Test #4 (Fig. 4)) with the ^{137}Cs source (30-y half-life) is used to check both detector uniformity of response throughout the camera's 57.6-cm diameter FOV and that camera sensitivity remains constant. Detector uniformity is established from visual inspection to ensure that no lines or streaks due to problems with detector discriminators or PMTs are observed. Sensitivities are measured as counting rates per detector pair (K cps/detector pair) and should remain constant from day to day.

Finally, a 20-cm diameter cylinder uniformly filled with 0.5 mCi ^{18}F or ^{68}Ga is centered in the camera's FOV and a scan is acquired for a total of 30M cts (quality control Test #5 (Fig. 5)). This acquisition takes about 15 min, depending upon the Ga activity available. These data are reconstructed with all corrections applied to measure image nonuniformity across the central two-thirds of the image area. Nonuniformity is expressed as the percent standard deviation per pixel (SD across pixels divided by the average counts per pixel $\times$ 100). These values are tabulated. By requiring a fixed number of counts and summing planes over 4 cm, the constancy of image uniformity is determined. All 5 tests can be completed within 30 min before the first patient studies are started.

Clinical Protocols

The clinical protocols are described in Table 3. Prepreparation requires patients to fast for 4–12 h before imaging, women of childbearing age must have a negative pregnancy test, patients must give their consent, and patients must be weighed to calculate the amount of radiopharmaceutical to be administered. For FDG PET studies, a finger stick is used to draw a drop of blood to measure capillary blood glucose (CBG) with a hand-held glucometer. The CBG should fall in the 60–140-mg/dL range. In the event of elevated blood glucose levels, most often due to the patient eating in the hours before the

indicate correct operation of the PMTs. The quality control menu notifies the technologist of any problem with any PMT signal requiring manufacturer intervention.

The energy spectra (quality control Test #2 (Fig. 2)) collected from a line source at the center of the FOV are used by the camera software to calculate centroids and FWHM for the energy signals in each detector. The technologist inspects and records these values and compares them to the optimal energy centroids and FWHMs. This establishes the reliability of gain matching and power supplies to the detectors, since mismatched PMT gains will increase the summed signal width and any change in power supply voltage would change the peak

FIGURE 3. Summary of C-PET quality control. Examples of sinograms for a line source at 5 radial positions across the 25.6-cm transaxial field of view (FOV). These scans take 5 min to acquire and were taken at 1-wk intervals.

FIGURE 4. Summary of C-PET quality control. Left: Example of the sinogram from a blank scan with a ^{137}Cs point source. The dark crosshatches represent the gaps between the 6 detectors. Note the uniform appearance across the detectors. Right: Average counting rates in each of the 9 bank pairs (detector pairs in coincidence) plotted against days in a month. The error bars are the standard deviations across detectors.
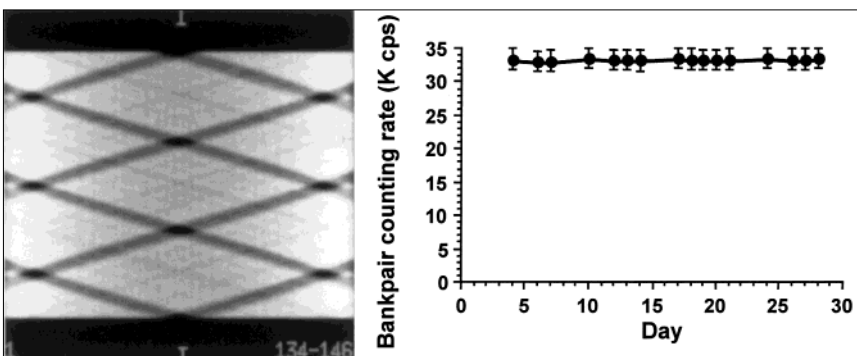
study, the patient may be asked to wait until blood glucose levels have returned to an acceptable range or to return at another time. It is important to minimize patient activity at the time of injection and during the delay between injection and scanning (uptake period) since this may cause FDG uptake into muscles, which can obscure and confound detection of subtle abnormalities. For example, a patient referred for assessment of a head and neck cancer should be asked to refrain from talking to minimize uptake in facial and vocal muscles. Similarly, a patient referred for study of a melanoma should be asked to refrain from walking and muscle flexing to minimize uptake in limb muscles.

Administered activity and delays between injection and scanning are summarized in Table 3. For torso surveys (the most common PET study) a 60–90-min delay is optimal. This allows normal and inflamed tissue uptake to plateau while tumor uptake continues to increase with time. Once the patient is positioned in the camera and patient information has been entered in the file manager of the acquisition terminal (Sun Ultra 60; Sun MicroSystems, Palo Alto, CA), the relevant predefined protocol is selected. For example, the patient is supine, feet first and arms raised for a 70-cm survey of the torso, from pelvis to neck. Five axial positions of emission scans are interleaved with 7 positions of transmission scans (extra transmission scans cover the edges of the axial FOV of the emission scans). Transmission source insertion/retraction (from the gantry housing) and changes in the discriminators and energy windows for transmission (610–880 keV) compared to emission (450–580 keV) are performed automatically. Study durations are summarized in Figure 6 and typical patient emission and transmission scan counting rates are shown in Figure 7. All C-PET studies include transmission scans over the entire axial range. Cardiac studies are performed by acquiring 20-min ^{13}N-ammonia scans (acquired from 3–23 min after injection) after activity has cleared the blood pool, followed by 20-min ^{18}F-FDG scans acquired from 20–40 min postinjection.

After the initial acquisition is completed, the patient may undergo a second emission sweep to survey the head and neck or lungs at a second time point. This is used to distinguish tumors (increasing uptake with time) from normal and/or inflamed tissue (no increase) (*15*). When metastases near the bladder are a concern, the patient may be asked to void and return for a postmicturation scan.

An initial (nonattenuation corrected) image is reconstructed using a reconstruction menu and predefined reconstruction protocol. This is used to determine that all areas of concern were imaged. Provided this was accomplished, the patient is allowed to leave. The technologist then draws elliptical regions on this image at 5–10 slices spaced across the axial extent of the study. These regions match the body outline as closely as possible, and are used for background subtraction. The fully corrected images (SUV images), with measured attenuation and dead-time correction and scatter and randoms subtracted, then are reconstructed. These fully corrected emission images and transmission images are checked for the absence of reconstruction artifacts and then transferred to the reading physicians for review and reporting. Hardcopy glossy films also may be generated for use by referring physicians and surgeons. The raw (sinogram and counting rates) files as well as reconstructed images then are archived for future use and referral. Image reconstruction typically takes less than 10 min for the uncorrected images and less than 30 min for the fully corrected images over 180×4 mm slices, using the workstation (Sun Ultra 60; Sun MicroSystems, Palo Alto, CA). Image transfer

FIGURE 5. Summary of C-PET quality control. Left: Transaxial view of the fully corrected image of a uniformly filled cylinder (4 M cts/slice). Right: Plot of percent standard deviation per pixel for these images plotted each day.
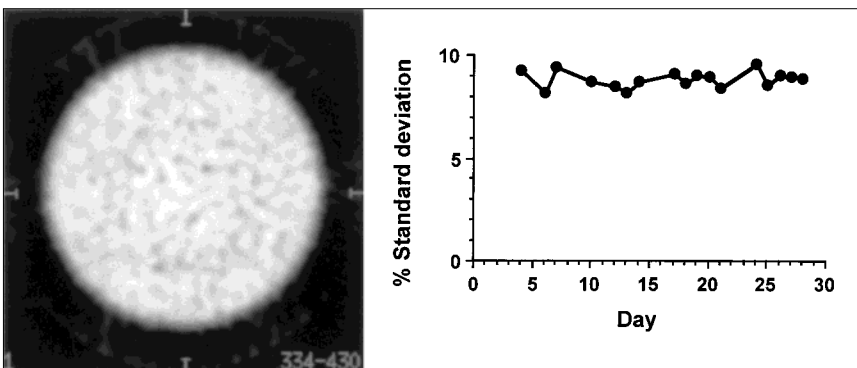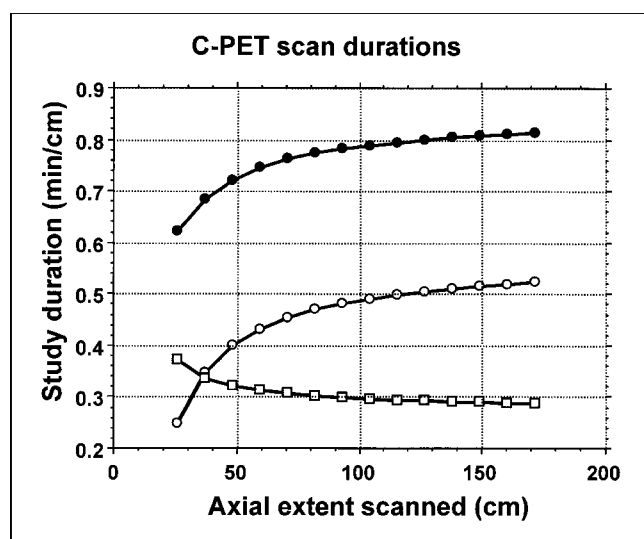
TABLE 3
Clinical Protocols

Study type	Indications	^{18}F-FDG activity administered	Delay (uptake) time	FOV	Duration	cm covered
Brain	Trauma, tumor, seizure	0.068 mCi/Kg	30–45 min	25.6 cm	30 min	25.6 cm
Head and neck	Cancer, follow-up	0.068 mCi/Kg	60–90 min	57.6 cm	55 min	48 cm
Torso	Cancer, follow-up	0.068 mCi/Kg	60–90 min	57.6 cm	55 min	70 cm
Cardiac (flow metabolism)	CABG, transplant work-up	0.068 mCi/Kg	30 min	57.6 cm	63 min	25.6 cm
Head-to-knees	Metastatic cancer	0.068 mCi/Kg	60–90 min	57.6 cm	85 min	115 cm

takes place before 5 pm in our PET center. This allows physician review at the end of the working day. Data sizes are fairly large: sinogram data for a 70.4-cm survey occupies 80 MB and image data occupies 20 MB of disk space (nonattenu-aton corrected and fully corrected emission data and transmission data) so that sinograms are compressed and data archived to optical disks (1-GB capacity) and 8-mm videotape (3-GB capacity).

Fully corrected images may be read as SUV images using the option in the LOAD and ROI (region of interest) modules provided with the C-PET camera. User-defined regions then may be overlain on the images to measure tumor and normal organ SUVs. These SUV values are used to discriminate between inflamed and tumor tissue, as described above (*15*), or to monitor tumor response to therapy over time. Finally, a DICOM conversion utility may be used to import, register and overlay CT or MRI images onto the PET images. These utilities increase the diagnostic power of the PET images.

RESULTS AND DISCUSSION

Figures 1 through 5 summarize typical results of C-PET quality control. Figure 1 shows the average baselines and standard deviations among baseline values, as well as average daily differences between individual PMT baselines acquired over a month. Baselines are the PMT signals in the absence of scintillation light in the detectors. Figure 2 shows the peak of a typical energy spectrum and plots the average centroid and FWHM of the detector energy spectra acquired over a month. Figure 3 shows the sinograms from line source data at weekly intervals over a month. Figure 4 shows an example of a ^{137}Cs single-photon blank scan and a plot of the average counting rate per bank pair (detector pair in coincidence) from a month of data. Finally, Figure 5 shows an example of the fully corrected emission image of a uniformly filled cylinder and plots the percent standard deviation (sd/mean $\times$ 100) across pixels in these images. Notice the constancy of these values indicating the stability of the camera system. Changes of $> 3\%$–5% would indicate problems requiring attention.

Figure 8 shows an example of a torso study from the C-PET camera. Shown are transaxial, sagittal and coronal views of the fully corrected and transmission images from a patient with
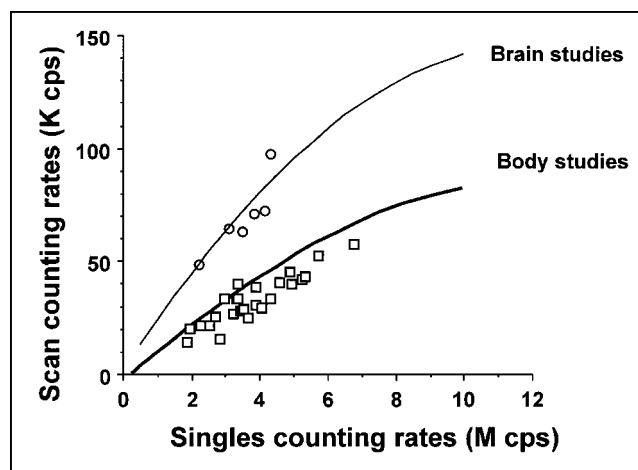

FIGURE 6. Scan durations for the C-PET camera against axial extent covered (scan length). Emission scans are 0.55 min/cm (open circles) and transmission scans are 0.25 min/cm (open squares) resulting in a typical study duration of 0.8 min/cm on average (closed circles). For a 70-cm study, which is typical for a cancer follow-up study, the transmission study will take 0.46 min/cm. The total time will be 0.77 min/cm or 54 min. Typical values given here are the calculated average.

FIGURE 7. Typical patient counting rates: these are typical emission counting rates for brain (open circles) and body (open squares) studies using the C-PET camera. Counting rates averaged 37 K cps for body studies and 53 K cps for brain studies. The 37 K cps was averaged over more than 200 patients. Typical transmission scan counting rates are 210 K cps (180–240 K cps).
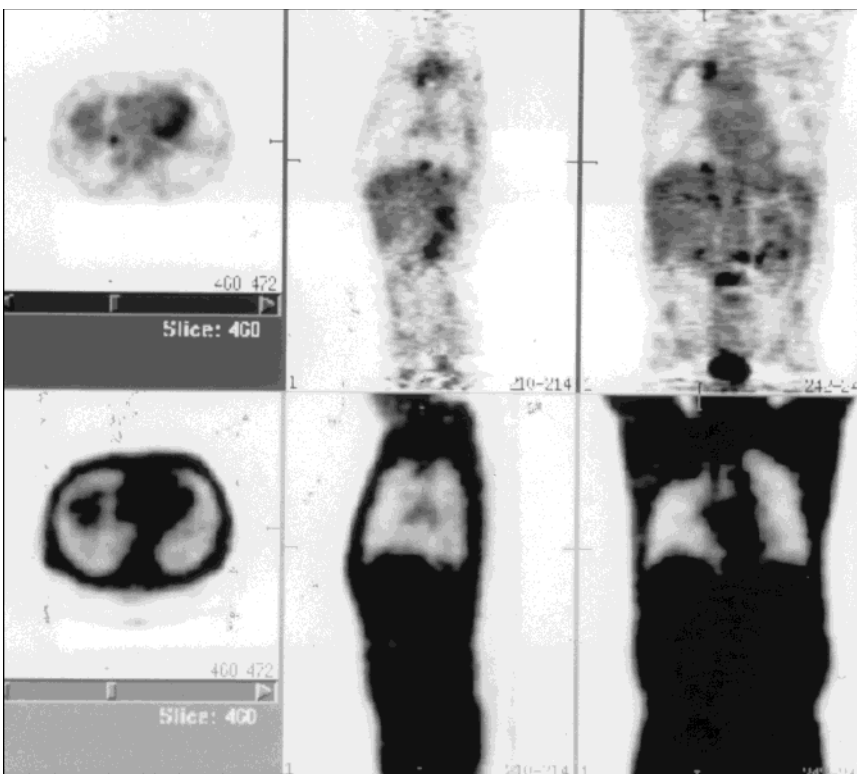
FIGURE 8. Torso study of a 62-y-old man with right lung pancoast tumor who was evaluated for metastases after chemotherapy and radiation therapy. 4.8 mCi/74 kg ^{18}F-FDG were injected. After an uptake period of 69 min, 70 cm were scanned in 63 min. Upper panels are transaxial, sagittal and coronal views of fully corrected (SUV) emission images and lower panels are transmission images. Residual disease was found at the primary site involving the apex of the right lobe. In addition, increased uptake was seen at the base of the right lung, in L3 and L4, and at 3 other sites, indicating tumor metastases. The right upper lobe tumor had an SUV of 5.1 and a diameter of 1.4 cm. The tumor at the base of the right lobe had an SUV of 4.8 and a diameter of 1.4 cm. Normal tissue SUVs in this patient were 0.5 for the lung and 2.2 for the liver.

lung cancer. FDG PET torso surveys comprise 70% of our PET studies, with solitary pulmonary nodule cases alone comprising 30% of studies. Similar image qualities are available for brain, head and neck, cardiac (^{18}F-FDG and ^{13}N-ammonia) and head-to-knees surveys. In all cases no study lasted longer than 90 min and all were fully reconstructed within 1 h of completion.

The C-PET camera allows an efficient throughput of patients with studies lasting from 30 min (brain and FDG cardiac) to 60 min (torso and head-and-neck studies) to 90 min (head-to-knees surveys). The simplicity of operation (automated and menu-driven), rapidity, accuracy and quality of studies, allows 1 or 2 technologists to perform 8 PET studies a day. The disadvantage of this system is that no on-line randoms subtraction is available currently. The use of profile subtraction using elliptically defined regions, however, works well in 95% of patient studies. For particularly obese patients or studies with particularly high single-photon counting rates, a no-background-subtraction option may be used to generate less noisy images, albeit with reduced contrast. An on-line randoms subtraction method and improved scatter subtraction are being addressed by the camera manufacturer.

CONCLUSION

The C-PET camera is easy to operate, uses 1-h protocols to survey the body, and is capable of all clinical PET studies. The large axial FOV, postinjection singles transmission capability, and menu-driven acquisition and processing make it an attractive camera for clinically oriented PET centers or services.

REFERENCES

1. Rigo P, Paulus P, Kaschten BJ, et al. Oncological applications of positron emission tomography with fluorine-18 fluorodeoxyglucose. *Eur J Nucl Med.* 1996;23:1641–74.
2. Hoh C K, Schiepers C, Seltzer MA, et al. PET in oncology: will it replace the other modalities? *Semin Nucl Med.* 1997;27:94–106.
3. Brix G, Zaers J, Adam LE, et al. Performance evaluation of a whole-body PET scanner using the NEMA protocol. *J Nucl Med.* 1997;38:1614–1623.
4. DeGrado TR, Turkington TG, Williams JJ, et al, Performance characteristics of a whole-body PET scanner. *J Nucl Med.* 1994;35:1398–1406.
5. Townsend DW, Wensveen M, Byars LG, et al. A rotating PET scanner using BGO block detectors: design, performance and applications. *J Nucl Med.* 1993;34:1367–1376.
6. Karp JS, Muehllehner G, Geagan MJ, et al. Whole-body PET scanner using curve-plate NaI(Tl) detectors [Abstract]. *J Nucl Med.* 1998;39:50P.
7. Nelleman P, Hines H, Muehllehner G, et al. Performance characteristics of a dual headed SPECT scanner with PET capability. *IEEE Med Imaging Conf Rec.* 1995;1751–1757.
8. Martin WH, Delbeke D, Patton JA, et al. Detection of malignancies with SPECT versus PET, with 2-[fluorine-18]fluoro-2-deoxy-D-glucose. *Radiol.* 1996;198:225–231.
9. Simcic V, Rempel TD, Carhart C, et al. Performance characteristics of Siemens ECAM [Abstract]. *J Nucl Med.* 1999;40:282P.
10. Karp JS, Muehllehner G, Mankoff DA, et al. Continuous slice PENN-PET: a positron tomograph with volume imaging capability. *J Nucl Med.* 1990;31: 617–627.
11. Smith RJ, Hustinx R, Adam LE, Karp JS. Clinical performance of the CPET camera [Abstract]. *J Nucl Med.* 1999;40:280P.
12. Smith RJ, Karp JS, Muehllehner G, et al. Singles transmission scans performed post-injection for quantitative whole-body PET imaging. *IEEE Trans Nucl Sci.* 1997;44:1329–1335.
13. Smith RJ, Karp JS, Benard F, et al. A comparison of segmentation and emission subtraction for singles transmission in PET. *IEEE Trans Nucl Sci.* 1998;45:1212–1218.
14. Kilroy KJ, Riggin SL, Meehan DA, et al. Clinical PET protocols using the CPET camera [Abstract]. *J Nucl Med Technol.* 1999;27:166.
15. Hustinx R, Smith RJ, Benard F, et al. Dual time point FDG PET: a potential method to differentiate malignancy from inflammation and normal tissue in the head and neck. *Eur J Nucl Med.* 1999;26:1345–1348.